Journal of Southeast University (English Edition) Vol. 28, No. 1, pp. 64 - 72 Mar. 2012 ISSN 1003—7985

Mechanical performance evaluation of a new type of cable-stayed beam-arch combination bridge based on field tests

Ma Wengang Huang Qiao Chen Xiaoqiang Ren Yuan

(School of Transportation, Southeast University, Nanjing 210096, China)

Abstract: In order to study the mechanical performance of a new type of cable-stayed beam-arch combination bridge, the results of field static and dynamic load tests are comparatively analyzed with numerical results based on the Jingyi bridge straddling the Daxi River in Yixing. First, the test scheme, tasks, the corresponding measure method, as well as the relevant codes are described. Secondly, two sets of three-dimensional finite element models are established. One is Ansys which uses the solid element and the other is Midas which adopts the beam element. Finally, the experimental and analytical results are comparatively analyzed, and they show an agreement with each other. The results show that the bridge possesses adequate load-carrying capacity under all static load cases, but the capacity of dissipating external input energy is insufficient due to the relatively smaller damping ratio. The study results can provide a reference for further study and optimization of this type of bridge. Calibrated finite-element models that reflect the real conditions can be used as a baseline for future maintenance of the bridge.

Key words: arch bridge; cable-stayed bridge; vertical load; field test; three-dimensional model

doi: 10.3969/j.issn.1003-7985.2012.01.012

As in every work of art, many of the aesthetic qualities of a beautiful bridge are found in its format, and it is precisely in the format where the bridge designer can give it beauty[1]. The aesthetic functions and symbolic values of structures are more and more important, particularly when built in urban zones[2]. Bridge aesthetics is a part of the aesthetic of the environment that surpasses the territorial limitations of the surrounding environment. The aesthetic requirement boosts a considerable development of the beam-arch combination bridge.

In general, compared to the development of a new type of bridge or the complex structure, the correlative research is lagging behind the requirements of engineering construction. Fortunately, field tests have become a reliable means to provide a much more accurate estimate of the mechanical performance of a structure. Ref. [3] relied on field dynamic tests to test a newly developed lightweight fiber-reinforced polymer bridging system to meet the US military needs. They are also used to assess the Alfred Zampa Memorial Bridge, the first suspension bridge in the United States, with an orthotropic steel deck, reinforced concrete towers, and large-diameter drilled shaft foundations[4] as well as the Shenley Bridge, the first bridge application of the sandwich plate system technology in North America[5]. Field tests can also be used to analyze structural decay[6]. Even though analytical studies are becoming less expensive and allow for a faster introduction of new design improvements and maintenance decisions, actual field tests are still the most reliable sources of information and the only method of final validation of analytical studies[7]. Research has shown that analytical bridge evaluation procedures tend to underestimate the true stiffness and overestimate the response of steel girder bridges[8] owing to conservative assumptions often made to account for uncertainties in numerical analysis.

This paper presents the procedure and results of static and dynamic loaded field tests with the intention of understanding the mechanical performance of a new type of bridge with a graceful shape. The main contents of the field load tests include: 1) Observing the displacements of concrete and steel decks under test truck loads; 2) Checking the strains of the steel and concrete deck of key sections; 3) Testing the cable force under the design load; 4) Monitoring the displacement of the steel arch pylon during the entire field test. Two sets of three-dimensional finite element models are established and applied to calculate the bridge response. One is Ansys which uses the solid element and the other is Midas which adopts the beam element.

1 Bridge Description

The Jingyi Bridge is a double-set arch pylon cable-stayed bridge located in Yixing city of Jiangsu province. The bridge was built in 2009, carrying four-lanes for a main artery and two-lanes for an auxiliary road. It is a three-span bridge with a span combination of 28 m + 39 m + 106 m. The pylons consist of an intercrossing main arch pylon and an auxiliary arch pylon (see Fig. 1), and a set of steel tension rods are used for connecting the two. The main and auxiliary arch pylon are all of steel structure constructed with octagon steel box sections with

Received 2011-11-09.

Biographies: Ma Wengang (1980—), male, graduate; Huang Qiao (corresponding author), male, doctor, professor, qhuanghit@126.com.

Citation: Ma Wengang, Huang Qiao, Chen Xiaoqiang, et al. Mechanical performance evaluation of a new type of cable-stayed beam-arch combination bridge based on field tests[J]. Journal of Southeast University (English Edition), 2012, 28(1): 64 - 72. [doi: 10.3969/j.issn.1003-7985.2012.01.012]

curved stiffeners along the arch pylon and a chamfered circular-arc. The height of the main pylon is 73.6 m with an inclination of 8°, while the auxiliary pylon is 61.7 m with an inclination of 17° in the opposite direction. There are 16 pairs of stayed cables arranged on the bridge. The cable distance is 9 m on the steel box of the main span, and 6 m on the concrete box of the side span. The distance is 2.2 to 2.6 m on the arch pylon. The width of the steel deck is 51 m with two cantilevered pedestrian decks and the concrete girder is 27 m wide. The local combination zone of the main arch pylon and the auxiliary arch pylon is a steel box which is 58 m wide at the top, and the bottom plate is 45.5 m wide. The beam of both the concrete girder and the steel box are 2.5 m deep at the centerline, with a 1.5% transverse slope.

Fig. 1 Pictures of the Jingyi Bridge

2 Static Load Tests

The live load tests of the Jingyi Bridge were performed under both static and dynamic conditions after nearly one year in service. According to the code and the test method for large span concrete bridges, the main structure of the Jinyi Bridge was calculated at the following key points which were selected as crucial sections to carry out load tests for studying the static mechanical performance of the bridge: the section beyond the auxiliary pier (*A-A*), the middle span section of the concrete span (*B-B*), the section of the main span intersecting with the auxiliary pylon (*C-C*), the maximum positive bending moment sections of the main span (steel box span, section *D-D*), the section of the main pylon intersecting the steel box (*E-E*), the maximum bending moment section of the main pylon (*F-F*), and the maximum bending moment section of the auxiliary pylon (*H-H*) (see Fig. 2). In addition, the maximum longitudinal displacement of the main arch pylon at the tower top, the maximum deformation of the main span and the auxiliary span, and the cable force were also given concern in relevant load cases.

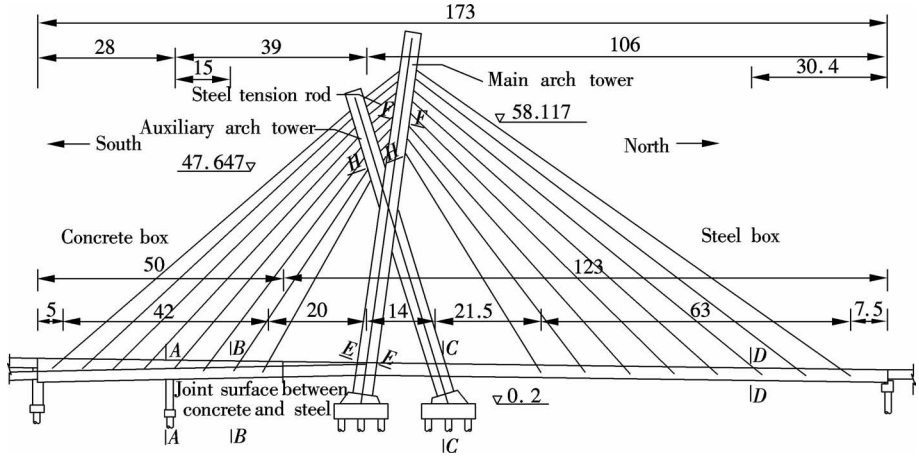

Fig. 2 Bridge vertical section (unit: m)

2.1 Measuring point arrangement

There are four key sections chosen for the main girder testing and three for the arch pylons, as shown in Fig. 2. The location of the strain transducer in each section is shown in Fig. 3.

According to the finite element analysis, the maximum deformation position of the main and the side spans can be determined. The specific locations are shown in Fig. 4.

2.2 Loading vehicle

Prior to testing, each vehicle was carefully weighed to obtain both the gross weight of the vehicle and the load at each axle. The three-axle dump trucks were loaded with gravel, of which the average weight for the front, middle and rear axles were 87.2, 122.5 and 122.5 kN, respectively. Furthermore, the average gross weight measured in the static field tests was 332.3 kN. The axle spacing of each dump truck was carefully measured at the nearby weight station before it was moved to the bridge. There were 20 dump trucks employed in the field tests, two of which were reserved in case of a possible accident or unforeseen malfunction.

2.3 Description of load cases

The longitudinal truck position is determined to produce the maximum live load action at the control section

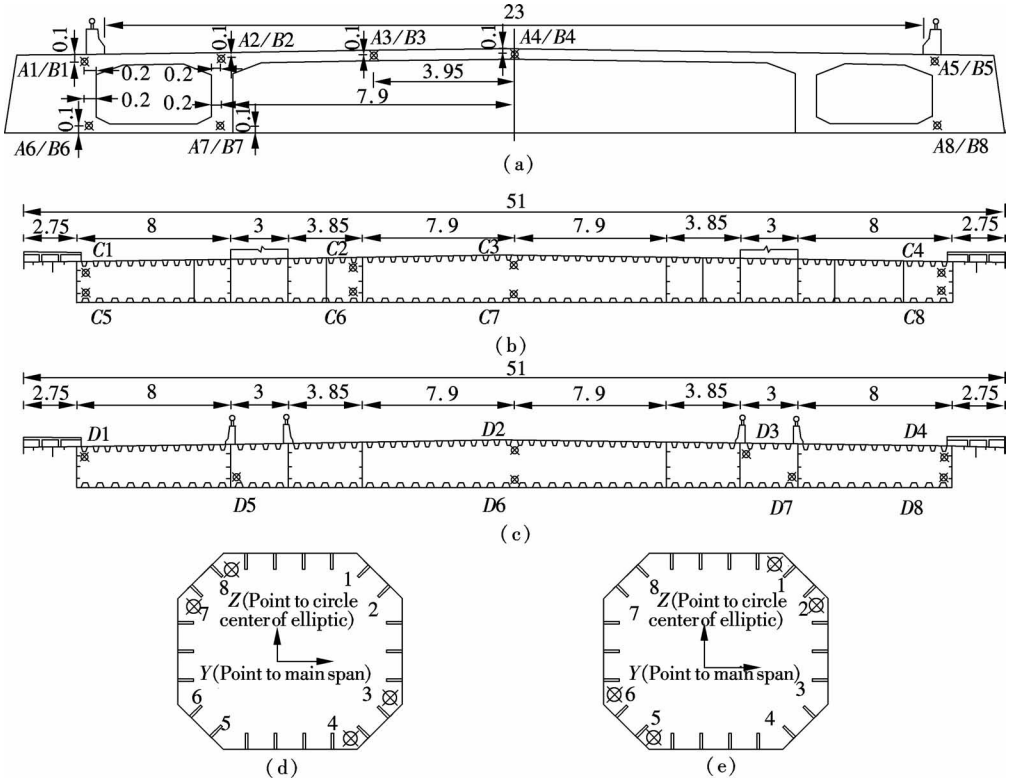

Fig. 3 The location of transducer (unit: m). (a) Sections *A-A* and *B-B*; (b) Section *C-C*; (c) Section *D-D*; (d) Section *E-E*; (e) Sections *F-F* and *H-H*

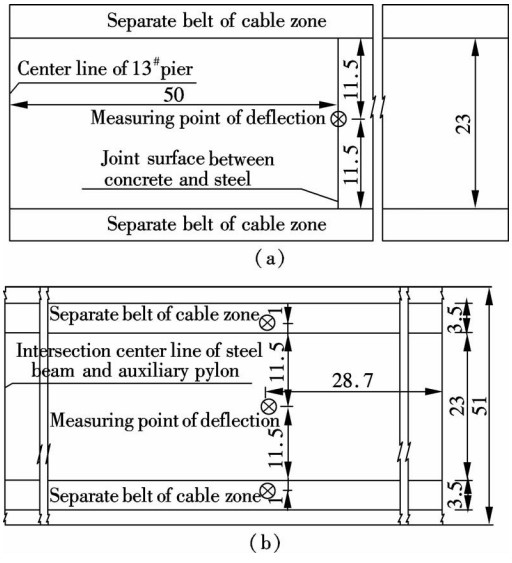

Fig. 4 The location of deflection measuring point (unit: m). (a) Defection measuring point of side span; (b) Defection measuring point of main span

under the test load case. Several testing items can be merged into one load case due to their similar shape of influence line and loading location, meanwhile satisfying the request of the test load efficiency. Finally, four load cases are determined to carry out the field tests. The details about the number of trucks and longitudinal as well as transverse locations of each load case are shown in Fig. 5.

Load case 1 contains the following: the maximum stress of section *D-D*, the mid-span deflection of the main span, the maximum cable force of the steel box side, the maximum stress of the main and the auxiliary arch pylons, and the longitudinal displacement of the main pylon included under the test loading of the maximum positive bending moments. Load case 2 also consists of a number of testing items: the stress of section *C-C*, the stress of the main and the auxiliary arch pylons, the deflection of the main span, the longitudinal displacement of the main pylon under the maximum negative bending moment. Since load case 3 can simultaneously concede the effects of the positive bending moment of section *B-B* and the negative bending moment of section *A-A*, in which the test items contain the stresses of section *A-A* and *B-B*, as well as the deflection of section *B-B*. Load case 4 is concerned with the response of the bridge under a partial load; furthermore, this case collects data for the further study of the shear lag of steel boxes and the large width-span ratio, just as in load case 1 and load case 2.

3 Dynamic Load Tests

The natural vibration characteristics of the bridge, which can reflect the holistic mechanical performance of the bridge, depend on the stiffness of the bridge and the mass distribution. The dynamic characteristics of the tests result in a much more thorough understanding about the operational state of the bridge. Two kinds of test modes are contained in the field test, namely, the barrier free running

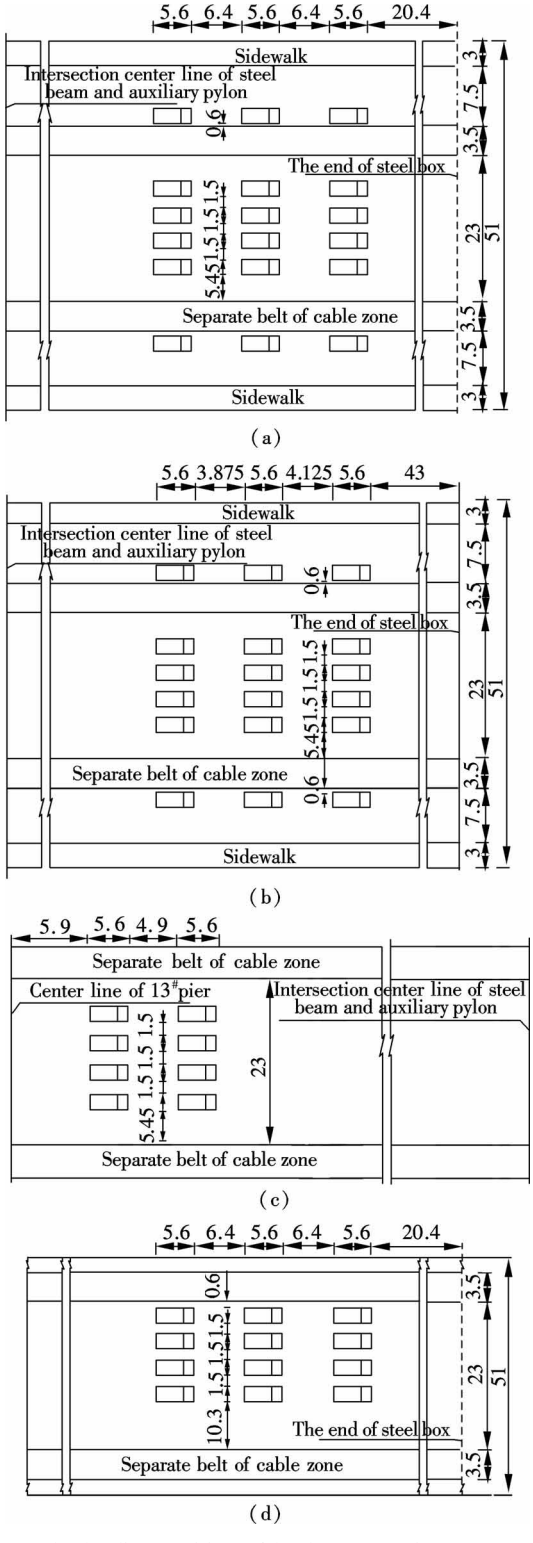

Fig. 5 The loading position of load cases (unit: m). (a) Load case 1; (b) Load case 2; (c) Load case 3; (d) Load case 4

test and the vehicle bump test.

3.1 Barrier free running test

Two dump trucks, each with a gross weight of 25 t, pass over the bridge with a uniform speed in the range of 5 to 55 km/h and an incremental speed of 5 to 10 km/h. The fastest crossing speed depends on the limitations of the engine performance as well as the driving skills of the drivers. A vibration pickup is installed on deck, which is connected to the data acquisition system and a laptop computer to collect and record the vibration responses under different speeds. The intention of the test is to acquire the impact factor of the structure and set up a correlation curve between the impact factor and the speed, and finally ascertain the most unfavorable vehicle speed.

3.2 Vehicle bump test

Prior to the test, a dump truck of 15 t in weight and a wooden plank of 150 mm in thickness and 150 mm in width are placed across the middle section of the main span, to enhance the bridge vibration. Before testing, the rear axle of the truck is placed on the wooden plank. Once the test begins, the rear axle of the truck is suddenly dropped from the plank to excite the bridge and to generate an instantaneous impact. Meanwhile, the vibration pickups are placed on the deck mid-span to collect the attenuation curve under the instantaneous impact, and to acquire the fundamental frequency and the damping ratio of the bridge.

4 3D Finite Element Analytical Model

The finite-element simulation is used to develop a better understanding and prediction of the global mechanical performance of the Jingyi Bridge. Fig. 6 illustrates the FE models of the tested bridge developed by computer calculation with the help of Midas using the 3D beam element and Ansys using the 3D solid element, the shell element, the link element and so on. Both the FE models, which represent the tested bridge in its as-built state, develop according to the bridge drawings. The main structural members of the bridge are stay cables, steel girders, concrete girders, and steel arch pylons, all of which are discretized by different finite element types in the two types of the model. The grillage model by Midas includes 21 truss elements for the steel tension rods, 32 tension-only elements for stay cables, and 271 beam elements for the remainder. The solid model is developed by Ansys, while 100 760 shell-63 elements are adopted to simulate the steel structure, and the concrete beam is divided into 118 948 solid elements (solid45). In addition, 8 736 link elements (link8) are used to imitate pre-stressed tendons, as well as 21 and 32 link elements (link8) for steel tension rods and stay cables, respectively. All the material properties used in the models stem from the relevant values recommended by the code for the design of highway reinforced concrete and prestressed concrete bridges and culverts, as shown in Tab. 1.

Tab. 1 The material properties used in models

Material	Elastic modulus/GPa	Poisson ratio	Density/(kg · m^{-3})
Steel	206	0.3	7 850
Concrete	34.5	0.2	2 500

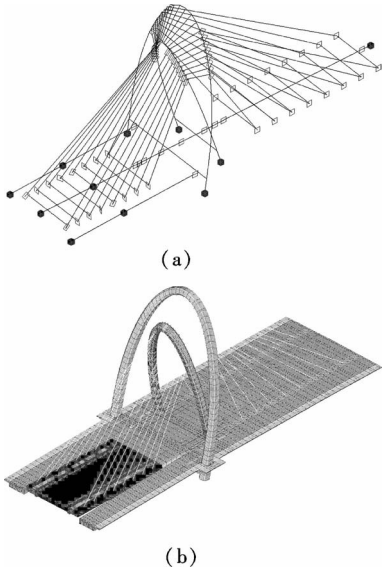

Fig. 6 Finite element analytical models. (a) 3D grillage model by Midas; (b) 3D solid element model by Ansys

5 Static Test Results

5.1 Load-strain curve of bridge deck

Using the calibrated 3D solid FE models, the concerned strain of different sections under the corresponding load case can be calculated and compared with the measured flexural strain, which is shown in Fig. 7. Comparing the measured strain with the calculated one, it can be found that the measured strain of the steel structure section is generally smaller than the calculated one, especially the measured strain of some individual points that are proved to be only half of the calculated one due to negligence of some local stiffness contribution (see Figs. 7(a) and (b)). The sub models are developed to study the local mechanical performance. Continued research is currently underway to study the shear lag about the large width-span ratio steel girder. From the comparison of the results in Fig. 7(c), it can be observed that the measured strain in the concrete box is much closer to the calculated results due to, on the one hand, the negligent contribution of the stiffness, and on the other hand, the much finer mesh generation for the solid65 element. Some measured strains on the concrete girders are much greater than the theoretical results, but converting the strain into the stress can reveal that the maximum stress in the concrete box is 6.6 MPa, which is much less than the request of the code for design of highway reinforced concrete and prestressed concrete bridges and culverts. According to the code, the allowable compressive stress of normal sections should not be greater than $0.5f_{ck}$ (= 16.2 MPa) during the service stage, where f_{ck} represents the standard value of the concrete axial compressive strength.

Through the same process, the maximum stress of the steel girder can be obtained. The peak values in the steel

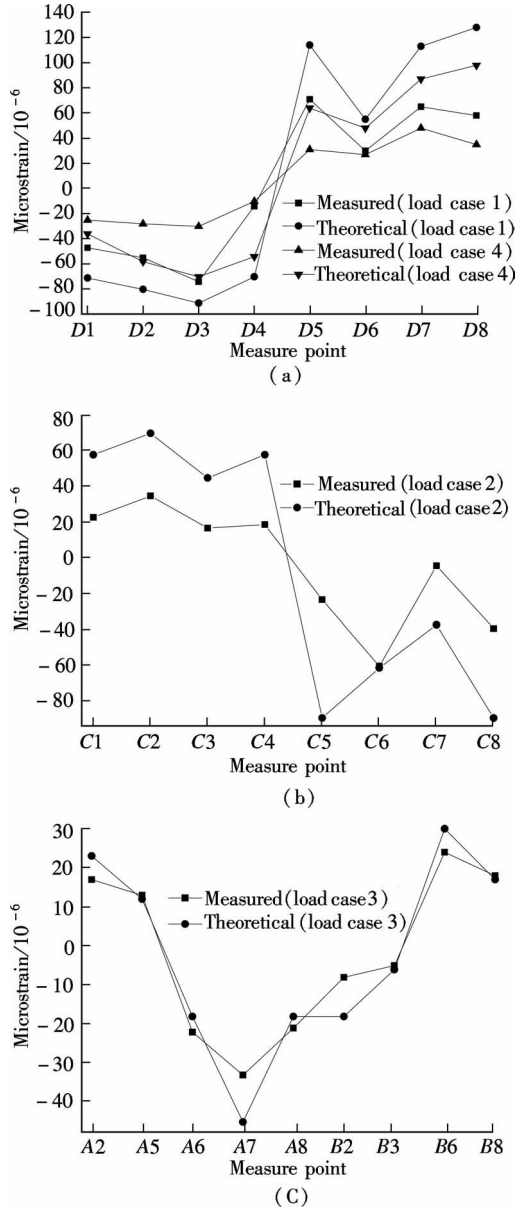

Fig. 7 Microstrain of sections under loading. (a) Section *D-D* under load cases 1 and 4; (b) Section *C-C* under load case 2; (c) Sections *A-A* and *B-B* under load case 3

girder are 54.6 and 53 MPa for tensile stress and compressive stress, respectively, which are only a quarter of the allowable bending stress of specifications for the design of steel structure and timber structure highway bridges and culverts. For the steel Q345 used for the steel structure of the Jingyi Bridge, the allowable bending stress is 210 MPa. Giving an overview about the stress, no matter what the measured values or the calculated results of the steel girder are, all reveal that the stress in the steel girder is quiet low, posing a potential for further optimization.

5.2 Load-strain curve of pylons

The results of the micro-strain about the main and the auxiliary pylons are shown in Fig. 8. From the above-

mentioned comparative results, it can be found that the measured results coincide much more with the calculated results. Given the relationship between the micro-strain and the stress, the maximum real tensile stress is 36.6 and 37 MPa for the main and the auxiliary pylon, respectively; and the compressive stress is 70.4 and 51.8 MPa, respectively. The above comparative analysis of the pylons illustrates that the design is excessively conservative only with regards to the static performance without considering the stability of the pylons. Some advice can be given for the optimization of the section size of the pylon based on further study of the mechanical performance considering the stability and including all the conditions during construction.

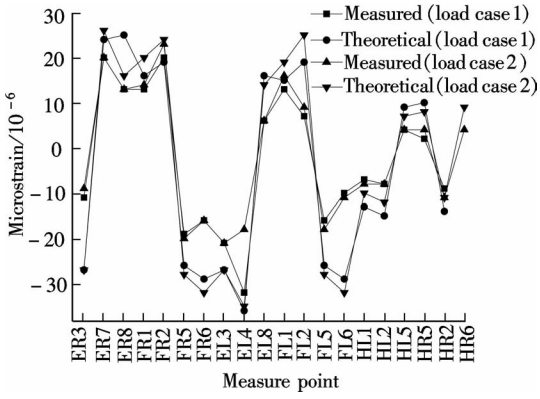

Fig. 8 Microstrain of pylons under load cases

5.3 Load-deformation curve of the girders

The deformation of the measured and the calculated values of the load cases are displayed in Fig. 9 (where ULC is the upstream-load case; CLC is the centerline-load case; DLC is the downstream-load case). The theoretical results by Ansys can give the specific points of deformation along the transverse section, while the Midas only gives the centerline results due to the inability of the grillage model considering the transverse deformation.

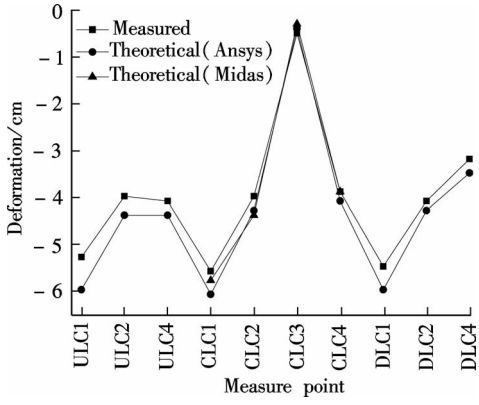

Fig. 9 Deformation of girder under load cases

According to the guidelines for the design of highway cable-stayed bridges, the maximum vertical deformation is not more than $L/400$ (L is the length of the main span) for the steel girder under lane loading (not including impact force). As shown in Fig. 9, the maximum measured deformation of the main span steel girder is 5.6 cm under the loading cases, which is much less than the allowable deformation $d = 108/400 = 0.27$ m. Clearly, the measured maximum girder deformation of the Jingyi Bridge, which can reveal that the bridge possesses the adequate stiffness, is far from the specification value, and it also proves the suggestion that the bridge possesses the potential for further optimization.

5.4 Load-cable force curve

By the two sets of validated models, it is possible to make sure that the maximum change of the cable force is focused on load cases 1 and 2. The changes in load cases 3 and 4 is relatively minor due to the much smaller vehicle loads. The measured and calculated cable force of load cases 1 and 2 are shown in Fig. 10 (where USSG is the downstream side of the steel girder; USSG is the upstream side of the steel girder).

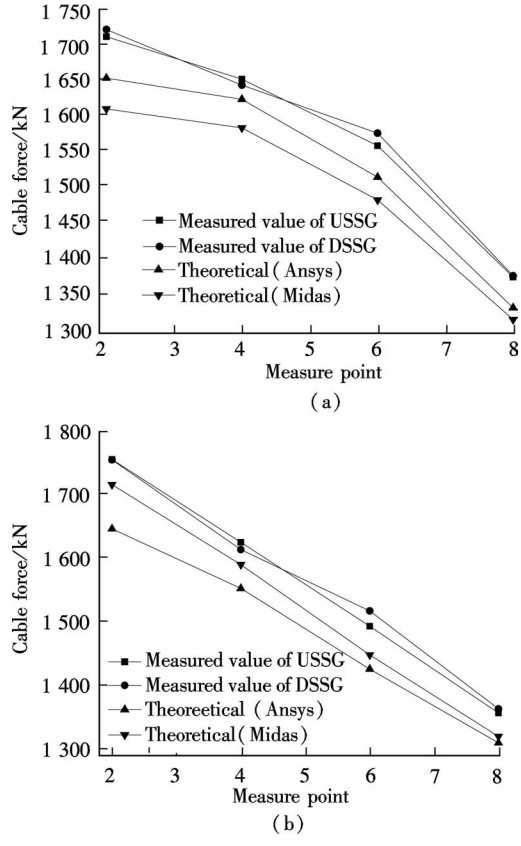

Fig. 10 The cable force under loading. (a) Cable force under load case 1; (b) Cable force under load case 2

It is worth giving attention to the cable force results, for which the measured values are generally greater than the calculated results, no matter whether by Midas or Ansys. It attributes to the damper installed between the cable and the girder, which has been installed before the field tests. The cable force based on the vibrating chord theory is

$$T = \frac{4wL^2 f_n^2}{n^2 g} \quad (1)$$

where n is the n-th vibration mode of the cable; f_n is the frequency of the n-th mode; L is the cable length; and w is the weight per unit length of the cable.

The effective length and the natural frequency of the cables are the important parameters in the application of the vibrating chord theory, which significantly affect the accuracy of the prediction of cable forces[9]. The instrument used to measure the natural frequency is validated, possessing enough precision in many similar fields or laboratory tests, so the cause which leads to much larger measured results focuses on the effective length of the cable. Continued research is currently underway to study the effective length based on the twice-equivalent cable length, which can consider the effects of the damper. So herein still gives the measured results without considering the effects of the damper. Although the measured values are much greater than the calculated results, the maximum cable force safety factors of the main and the auxiliary spans are 3.34 and 2.92, respectively. Both are greater than the 2.5 that is required by the guidelines for the design of highway cable-stayed bridges. So it is reasonable to consider that the cable is safe.

5.5 Longitudinal displacements of main arch pylon

The displacement of the main arch pylon is another important parameter which should be given special attention to during the experiment. Since the safety of the pylon is very important to the safety of the whole bridge, two sets of instruments based on different surveying principles are fixed to real-time monitor the displacement of the main arch pylon during the field tests to ensure the structural safety. The maximum measured values by the two sets of instruments and the calculated results using two sets of models are listed in Tab. 2.

Tab. 2 Measured and calculated tower top displacement of main pylon cm

Load case	Measured data		Calculated value	
	Total station	IBIS-S	Ansys	Midas
1	2.1	2.0	2.4	2.2
2	1.8	1.7	2.0	1.8

Comparing the measured values with the calculated values, it can be concluded that the main arch pylon is always in the safety state during the whole experiment. From another side, it is reasonable to believe that abnormal condition does not exist during the field test.

6 Dynamic Test Results

6.1 Fundamental frequency and damping ratio

There are many different analysis procedures that have been developed to extract the modal characteristics of structures. The two main subsets of procedures include the time domain and the frequency domain methods. Time domain methods produce modal characteristics directly from the structural response records in the time domain. Frequency domain methods accomplish the same tasks by converting the response signals into the frequency domain. As shown in Fig. 11(a), the time domain is obtained by the DH5923, and the corresponding measured natural frequency is 1.17. To ensure the accuracy of the measured fundamental frequency, another set of instruments IBIS-S are used and we acquire a result of 1.18 as shown in Fig. 11(b). With the help of Ansys, the theoretical fundamental frequency 1.167 can be obtained (see Fig. 11(c)). With reference to relative research, the average normal frequency of a human walking is between 1.6 and 2.4 Hz[10], so it can be considered that the

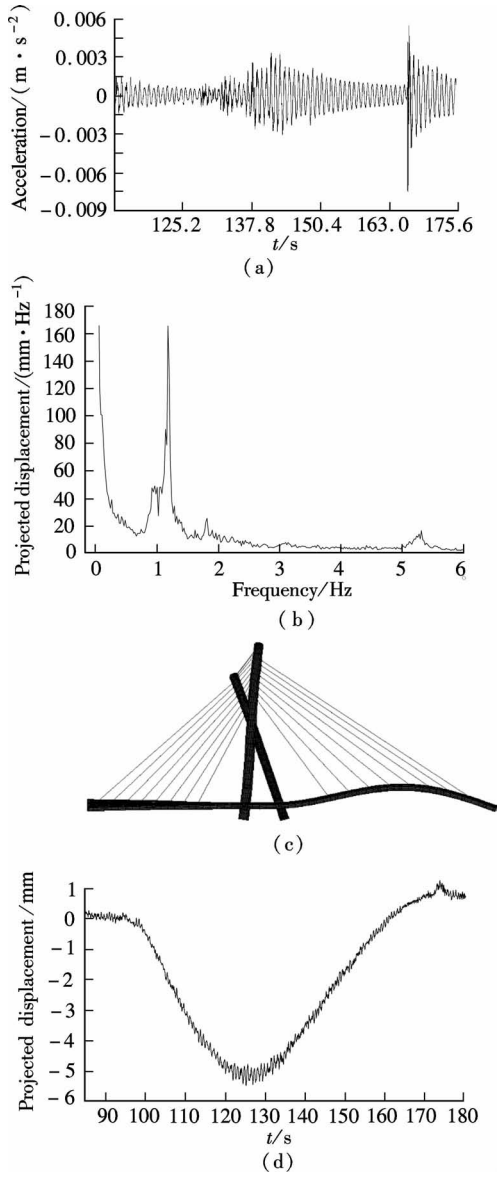

Fig. 11 The results of dynamic test. (a) Spectrum analysis under the load case of vehicle bump by DH5923; (b) Spectrum analysis under the load case of vehicle bump by IBIS-S; (c) Theoretical calculation of fundamental frequency by Ansys; (d) Dynamical deformation analysis of running test by IBIS-S at 22.2 km/h

resonance phenomenon induced by humans will not happen.

At the same time, the damping ratio of the bridge is acquired utilizing the time domain measured by the DH5923 (see Fig. 11 (d)). The measured value of 0.009 2 is much less compared with the general bridge damping ratio of 0.01 to 0.08. It can be thought that it possesses a much poorer ability to dissipate the external input energy from the seismic load.

6.2 Vehicle-induced impact tests

An amplification of the internal force is observed compared with the equivalent statically applied load when a bridge is subjected to a moving vehicle load. This increase is an essentially dynamic amplification of the static live load. Knowledge of the dynamic impact factors is important for an accurate determination of the ultimate load capacity and performance assessment of constructed bridges[7]. The objective of this load case is to evaluate the variety of bridge impact factors under different realistic speeds in order to collect information for the decision-making process. This study investigates the dynamic impact loads of track and wheel vehicles at different crossing speeds to increase the understanding of the appropriate impact factors used in the design[3].

As shown in Fig. 12, the impact factors under different speeds and in two directions are obtained by the analyses of the steel main girder's dynamic deflection, which are also detected by the IBIS-S, meanwhile, giving a regression analysis result.

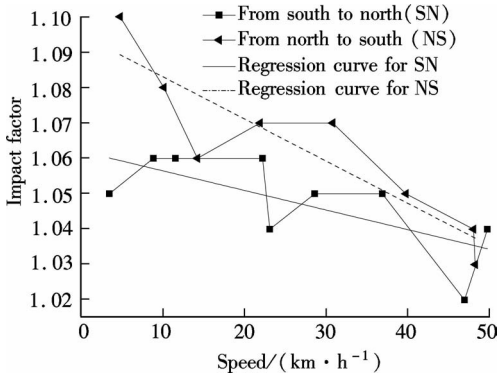

Fig. 12 Measurement and analysis of impact factor

Fig. 12 reveals that the impact load for the bridge is sensitive to vehicle speed with observed maximum impact factors as high as 1.10. Based on the analysis of the measured results and the regression curves, a conclusion can be drawn that the impact factor of vehicles moving from north to south is generally larger and also more sensitive than that in the opposite direction. The reason can be attributed to the uphill sector, causing the engines of vehicles to produce much more vibration. It is also found that the impact factor gradually decreases with the increase in vehicle speed in both directions.

According to the general code for the design of highway bridges and culverts, the impact factor should be calculated in the design as follows:

1) When $f < 1.5$ Hz, $\mu = 0.05$;

2) When $1.5 \text{ Hz} \leqslant f \leqslant 14$ Hz, $\mu = 0.176\,7 \ln f - 0.015\,7$;

3) When $f > 14$ Hz, $\mu = 0.45$.

The impact factor, which is adopted to be 0.05 in the design, is smaller than the field testing results. So it is reasonable to suggest that further study should be carried out to research the impact factor for this type of bridge, as well as for the code.

7 Conclusions and Suggestions

The Jingyi Bridge is a new type of stayed-cable beam-arch combination system, so there is not any mature theory or precedent that can provide reference. Field tests not only play an important role for the Jingyi Bridge itself, but also collect useful information for the further research of this type of bridge. Based on field testing of key sections and two sets of calibrated 3D FE models, several conclusions can be drawn from the obtained experimental data, resulting in some recommendations for similar designs and the design code.

1) In all the load cases, the measured strain, no matter whether it is in girders or in pylons, satisfies the requirement of the current design codes and shows a much smaller value compared with the finite-element model. This indicates that the bridge possesses an adequate strength to resist the service-level loads and also implies that the size of the bridge structure can be further optimized.

2) The results of the measured deflections of girders and the horizontal displacement of the pylons show a good agreement with the calculated results, and it also meets the requirement of the codes used in design. The deformation can completely recover after each unloading. All of this demonstrates that the bridge possesses adequate stiffness and works in the elastic stage.

3) Although the measured cable force is very conservative due to the lack of consideration of the damper effect, the safety factors of the cable is much higher than the requirements of the code. It can secure the idea that the cable is indeed safe under the service loads.

4) The results from the impact study demonstrate that the value used for this type is on the unsafe side according to the code, although the design of this bridge is quite conservative. The small damping ratio allows the bridge a poorer ability to dissipate the external input energy.

5) The finite-element analyses reasonably predict relatively accurate results as compared with the corresponding values under service-level moving loads. This once again asserts that the two sets of the FE models are precise enough to reflect the real conditions and can be used as a baseline for future maintenance of the bridge.

References

[1] Burke M P Jr. Bridge aesthetics: world view [J]. *Journal of Structural Engineering*, 1995, **121**(8): 1252 - 1257.

[2] Galvín P, Domínguez J. Dynamic analysis of a cable-stayed deck steel arch bridge [J]. *Journal of Construction Steel Research*, 2007, **63**(8): 1024 - 1035.

[3] Robinson M J, Kosmatka J B. Experimental dynamic response of a short-span composite bridge to military vehicles [J]. *Journal of Bridge Engineering*, 2011, **16**(1): 166 - 170.

[4] Cont J P, He Xianfei, Moaveni B, et al. Dynamic testing of Alfred Zampa Memorial bridge [J]. *Journal of Structural Engineering*, 2008, **134**(6):1006 - 1015.

[5] Harris D K, Cousins T, Murray T M, et al. Field investigation of a sandwich plate system bridge deck [J]. *Journal of Performance of Constructed Facilities*, 2008, **22**(5): 305 - 315.

[6] Potisuk T, Higgins C. Field testing and analysis of CRC deck girder bridge [J]. *Journal of Bridge Engineering*, 2007, **2**(1): 53 - 63.

[7] Kwasniewski L, Whkezer J, Garry Roufa P E, et al. Experimental evaluation of dynamic effects for a selected highway bridge [J]. *Journal of Performance of Constructed Facilities*, 2006, **20**(3): 253 - 260.

[8] Barker M G. Quantifying field-test behavior for rating steel girder bridge [J]. *Journal of Bridge Engineering*, 2001, **6**(4): 254 - 261.

[9] Fang I-K, Chen C-R, Chang I-S. Field static load test on Kao-Ping-Hsi cable-stayed bridge [J]. *Journal of Bridge Engineering*, 2004, **9**(6): 531 - 540.

[10] Jian F L, Wu D J, Li Q. Human-induced vibration analysis of pedestrian suspension corridor in Shanghai Hongqiao station [J]. *Journal of Vibration and Shock*, 2010, **29**(8):136 - 140. (in Chinese)

基于现场试验的新型斜拉-梁拱组合体系桥梁力学性能评估

马文刚 黄 侨 陈晓强 任 远

(东南大学交通学院,南京 210096)

摘要:为了研究新型斜拉-梁拱组合体系桥梁的力学性能,以跨越宜兴大溪河的荆宜大桥为对象,对现场静、动载作用下结构的实测反应与相应的数值计算结果进行了对比分析研究. 首先,给出了试验方案、任务、相应的测试方法及引用的相关规范;然后分别建立了三维 Ansys 实体模型和三维 Midas 杆系模型;最后,对比分析了模型计算结果与试验测试结果,两者吻合良好. 研究表明:该桥在各静载工况下均具有足够的承载力;在动载作用下,实测阻尼比相对较小,结构耗散外部输入能量的能力偏低. 研究成果可为对该类结构进一步研究和优化提供参考,同时经试验修正的、准确的计算模型可以作为该桥营运后维修、加固的基准模型.

关键词:拱桥;斜拉桥;竖向荷载;现场试验;三维模型

中图分类号:U443.38;U448.27